New Criteria for Selecting Reliable Thellier-Thellier type Paleointensity Results from the 1960 Kilauea Lava Flow, Hawaii

Doohee JEONG
Southern University of Science and Technology
Qingsong Liu (qsliu@sustech.edu.cn)
Department of Ocean Science and Engineering, Southern University of Science and Technology
Yuhji YAMAMOTO
Kochi University
Yongjae YU
Chungnam National University
Xiang ZHAO
Australian National Universtiy
Huafeng QIN
Institute of Geology and Geophysics, Chinese Academy of Sciences

Full paper

Keywords: Thellier-Thellier experiment, Paleointensity, Domain state, Thermal alteration

Posted Date: November 6th, 2020

DOI: https://doi.org/10.21203/rs.3.rs-102488/v1

Version of Record: A version of this preprint was published at Earth, Planets and Space on July 16th, 2021. See the published version at https://doi.org/10.1186/s40623-021-01473-6.

Abstract

Thellier-Thellier type paleointensity experiments associated with partial thermal remanent magnetization (pTRM) checks have been widely used to determine paleointensity values from volcanic and archaeological media. However, previous studies further revealed that a substantial portion of paleointensity results with positive checks for historical lavas largely fails to predict the known Earth's field intensity values. To determine the fidelity of paleointesnity values, conventional Thellier-Thellier type paleointensity experiments have been performed from the Kilauea lava flows erupted in 1960. Our results show that positive pTRM checks range from 30.34±1.39 to 53.04±1.80 μT. This strongly indicates that positive pTRM checks can't guarantee the fidelity of paleointensity results especially when the unblocking temperatures for the newly-formed magnetic particles are higher than the treated temperature. Thus, in this study, to check thermal alteration during heating, the temperature-dependent of hysteresis parameter measured at the room-temperature for the thermally-treated samples were also measured. Our new results show that almost all biased paleointensity values correspond to B_{cr}/B_c >3 and CI >~10%, which indicates strong effects of domain state and thermal alteration on the fidelity of paleointensity results. Our study provides a feasible criteria to further improve the fidelity of paleointensity estimations.

1. Introduction

Variations in the Earth's magnetic field intensity at different time scales bear great information on the growth of Earth's deep interiors (Macouin et al. 2004; Tarduno et al. 2007; Biggin et al. 2015) and the evolution of geodynamo (Larson and Olson, 1991; Glatzmaier et al. 1999; Olson et al. 2013). There are two different types of approaches to trace the temporal variation of geomagnetic field intensity: relative paleointensity determination (RPI, Tauxe 1993) and absolute paleointensity determinations (Thellier 1938; Thellier and Thellier 1959). Sediments carry depositional or post-depositional remanent magnetization (DRM or pDRM), and are excellent media to records the semi-continuous RPI (Valet et al. 2005; Yamazaki and Oda 2005; Channell et al. 2009; Ziegler et al. 2011). In practice, volcanic rocks are suitable for high resolution spot-readings ancient geomagnetic field intensity determination.

Modern absolute paleointensity determinations require multiple step heatings with systematic alteration (or consistency) checks. The Thellier protocol (Thellier 1938; Thellier and Thellier 1959) was initially proposed to compare the destruction of thermoremanent magnetization (TRM) and acquisition of laboratory-induced partial thermoremanent magnetization (pTRM) at equal temperatures. Thellier-type double heating techniques have been slightly modified, with each method has pros and cons (Thellier 1938; Thellier and Thellier 1959; Coe 1967; Aitken et al. 1988; Yu et al. 2004). The most commonly used technique is the so-called "Coe" protocol (Coe 1967), in which we first heat the specimen to T_i in a zero-field to determine the NRM lost. To determine the pTRM gained, we second heat specimen to T_i in an in-field conditions. Aitken et al. (1988) modified the Coe method (1967) by reversing the order of double heating. The IZZI protocol alternates the Aitken method in odd steps and the Coe method in even steps (Yu et al. 2004). Detailed reviews of various Thellier-type techniques were provided by Valet (2003) and Biggin (2010).

Once the paleointensity determination is carried out, the results are displayed in an Arai plot (Nagata et al. 1963) where the slope of NRM remaining versus pTRM gained is the ratio of ancient to laboratory magnetic field intensity. Only the stable single-domain (SD) particles follow a linear Arai plots, reflecting identical spectrum of unbloking temperature (T_{ub}) and blocking temperature (T_b). Multi-domain (MD) and pseudo-single domain (PSD) grains tend to produce a non-linear (or sometimes zig-zagging) Arai plots (Dunlop and Özdemir 2001; Leonhardt et al. 2015; Paterson et al. 2015). Inequivalent T_{ub} over T_b is responsible for such a non-linearity in an Arai plot. To quantify undemagnetized pTRM for non-uniformly magnetized TRM, the pTRM tail check was introduced (Riisager et al. 2000; Riisager and Riisager 2001; Yu and Dunlop 2003). In addition to the physical origin, a chemical contribution can alter the linearity of an Arai plot. For instance, growing of newly formed magnetic particles by chemical transformations (Yamamoto 2006) can induce thermochemical remanent magnetization (TCRM).

The most convenient (yet the easiest) way to ensure the high fidelity of paleointensity determinations is to check the quality of paleointensity determination using historic rocks whose geomagnetic field intensity is readily known (e.g., IGRF-International Geomagnetic Reference Field). To this end, the reliability of absolute paleointensity determinations was tested using historic lavas from Hawaii, US (Tsunakawa and Shaw 1994; Chauvin et al. 2005; Oishi et al. 2005; Herrero-Bervera and Valet 2009; Morales et al. 2010; Cromwell 2015), Italy (Calvo et al. 2002), Japan (Tsunakawa and Shaw 1994; Yu 2012), Spain (de Groot et al. 2015; Calvo et al. 2016), and western US (Coe et al. 2004).

Among various historic sites, the 1960 historic lavas in Hawaii drew more attention because of its accessibility. However, relatively easier accessibility did not guarantee successful duplication of geomagnetic field intensity information. In fact, the 1960 lava often yielded biased paleointensity determination toward higher/lower values up to 10–20% (Tanaka and Kono 1991; Tsunakawa and Shaw 1994; Tanaka et al. 1995; Valet and Herrero-Bervera 2000; Hill and Shaw 2000; Yamamoto et al. 2003; Herrero-Bervera and Valet 2009; Morales et al. 2010). Origin of heterogeneous or anomalous paleointensity outcome possibly lies on the influence of thermochemical remanent magnetization (TCRM) (Yamamoto et al. 2003), on the presence of local magnetic anomaly (Morales et al. 2010), or alteration and neo-formation of magnetic particles during repeated heatings (Zhao et al. 2014).

The present study was designed to incorporate the temperature dependence of magnetic hysteresis as a potential alteration checker. We aim to determine the exact mechanisms for the biased paleointensity results with positive pTRM checks. This is extremely important for paleointensity determinations for older rocks.

2. Samples

As the largest volcano in the world, the Kilauea is located at 19° 3’ N, 204° 3’ E (Fig. 1). On January 13, 1960, eruption began along the east rift zone of Kilauea. The 1960 eruption lasted for about a month and the lava covered an area of 10 km^2 (Ritcher et al. 1970; Rowland and Walker. 1987). According to international geomagnetic reference field (IGRF- 1965) model, the geomagnetic field intensity at the

eruption site would be 36.2 μT. Paleointensity determinations have yielded results ranging from 33.55 to 53.5 μT (Tanaka and Kono 1991; Tsunakawa and Shaw 1994; Tanaka et al. 1995; and Yamamoto et al. 2003). For instance, Tanaka and Kono (1991) documented presence of two segments in an Arai plot. They picked lower temperature segment as pTRM checks failed at higher temperature ranges. As a consequence, paleointensity determinations were overestimated (Tanaka and Kono 1991).

A total of 30 cylindrical-shaped basaltic core samples collected. Paleointensity determinations were carried out using the IZZI-protocol. Stepwise double heatings were carried out in 12 steps at 200, 300, 350, 400, 450, 480, 500, 520, 540, 560, 580, and 600 ºC. We performed pTRM checks at 300, 400, 480, 520, and 560 ºC. A laboratory field of B_{lab} = 20 μT was used for all in-field step heatings.

3. Results

3.1. Rock magnetism

Magnetic hysteresis measurements were performed using a variable field translation balance (VFTB) with a saturation field of 1 T. Values of saturation magnetization (M_s), saturation remanence (M_{rs}), and magnetic coercivity (B_c) were calculated after removing paramagnetic portion. The coercivity of remanence (B_{cr}) were determined from stepwise backfield demagnetization measurement. At least one chip was used for 30 different basaltic cores. The magnetic hysteresis results are displayed on a Day-diagram (Day et al. 1977) according to the criteria of Dunlop (2002) (Fig. 2a). All the samples fell in the pseudo-single-domain (PSD) range (Fig. 2a). The squareness versus coercivity plot showed a linear correlation with a mean slope value of $\approx 0.01\ mT^{-1}$ (Fig. 2b).

The first order reversal curve (FORC) diagrams were also obtained (SF = 8), using an alternating gradient force magnetometer (MicroMag 2900). Results from the chip of A1 display closing and elongated contours, reflecting fine-grained nature (Fig. 3). It is common to observed vertical spreads on closed contours, indicating the presence of PSD (Fig. 3).

3.2 Paleointensity determination

Paleointensity determinations were accepted when they pass the following selection criteria: (1) demagnetization of NRM must be univectorial with maximum angular deviation (MAD) angles < 4° (Kirschvink 1980); (2) pTRM checks must agree with original pTRM within 5%; (3) the ratio of maximum difference produced by a pTRM check over the length of the best-fit line DRAT should be less than 10% (Selkin and Tauxe 2000); (4) the angle between the principal fractions anchored to and free from the origin DANG (Tauxe and Staudigel 2004) should be < 4°; (5) at least 6 data-points with more than 48% of extrapolated NRM fraction (Coe et al. 1978) must be included in regression analysis; (6) the degree of scatter about the best-fit line normalized by the estimated slope (York 1969) should be < 5%.

Paleointensity estimates were calculated from incline of the Arai plot (Fig. 4). Paleointensity estimates were calculated from slope of Arai plot, which ratio between ancient geomagnetic field and the applied

laboratory field. With these selection criteria, a total of 9 samples were successful paleointensity estimation (Table 1). The magnetization removed at 560 °C (< 10%) with a few exceptions. The paleoinensity results range from 30.34±1.39 to 53.04±1.80 μT. Although consistent in range of errors (10% of IGRF model≈36.1±3.61 μT), large value differed by more than 10% from expected values. This erroneously result such as high estimated paleointensity caused by production of thermochemical chemical remanent magnetization (TCRM) during heating proccese (Yamamoto et al. 2003).

Table 1
Paleointensity results from Hawaiian lava 1960.

Sample	μT (°C)	*n*	*f*	*g*	*q*	*B* (μT)
conventional paleointensity						
A1*	200–600	12	0.89	0.84	23.6	46.80 ± 1.48
A10	200–520	8	0.54	0.36	3.96	41.38 ± 2.04
A11	200–520	8	0.51	0.83	5.3	40.65 ± 3.22
A15	200–540	9	0.74	0.75	14.92	48.55 ± 1.80
B2*	200–600	12	0.54	0.32	5.52	44.84 ± 1.41
B5*	300–580	10	0.48	0.75	8.88	37.04 ± 1.15
B7*	200–540	9	0.59	0.69	8.8	30.34 ± 1.39
C6	200–500	7	0.71	0.75	15.86	53.04 ± 1.80
C7	200–520	8	0.71	0.53	5.54	49.94 ± 3.42
mean		9				43.62 ± 1.97
mean*		4				39.76 ± 1.35
recalculated paleointensity						
A1*	300–500	6	0.53	0.66	10.73	39.08 ± 1.29
A10			0.32	0.38	1.16	42.54 ± 4.53
A11			0.34	0.60	1.28	38.30 ± 6.17
A15			0.56	0.68	5.56	49.96 ± 2.43
B2*			0.21	0.44	1.92	32.49 ± 1.53
B5*			0.33	0.48	2.83	32.62 ± 1.81
B7*			0.25	0.67	1.78	30.72 ± 2.90
C6			0.49	0.54	4.6	51.83 ± 2.94
C7			0.49	0.25	1.57	40.97 ± 3.16
mean		9				39.83 ± 3.08
mean*		4				33.73 ± 1.88

μT is the temperature interval used in paleointensity estimation; n is the number of points used in paleointensity estimation; f,g, and q are NRM graction, gap factor, and quality factor of Coe et al., (1987). *is value meets the condition (B_{cr}/B_c <3, CI < 10%).

3.3 Temperature-dependent rock magnetic properties

The paleointensity results vary considerably by several factors. Non-linear feature in Arai plots can be caused either by MD effect or by thermal alteration during heating. In order to detect exact reason, sister samples were heated to the same paleointensity measuring heating steps (200, 300, 350, 400, 450, 480, 500, 520, 540, 560, 580, 600 ºC). Then after, hysteresis loops were measured at room temperature of each step to detect thermal effects (Henry et al. 2005). The room temperature normalized magnetic saturation remanence (Figure. 5) versus temperature. The feature of Mrs_T/Mrs_{room} can be divided into two groups from room temperature to 500 °C. The first group shows excluding low temperature relatively stable from 300 to 500 °C (Fig. 5a, e, f and g). The other group shows dome like feature (Fig. 5b, c, d, h and i). This feature mean that super-paramagnetic particles change to single domain particles or surface of pseudo single domain gained characteristic remanence magnetization at the 300 ~ 500 °C intervals. Under 300 °C points were considered to influence of VSM. This effect is reflected in the trend of TRM-NRM trend. Basis on this, a new interval from 300 °C to 500 °C was set up and estimation of paleointensity.

4. Discussion

The studied of lava flows was erupted in 1960 from Hawaiian volcano. All together, 9 of 30 samples yield paleointensity results with positive pTRM checks using the IZZI protocol. The mean value of paleointensity was ~ 43.6 μT, which is higher than the expected value from the study area (~ 36.1 μT). In addition, the paleointensity results range widely between 30.34±1.39 and 53.04±1.80 μT (Fig. 6).

Previous studies have already shown that positive pTRM checks don't really guarantee the fidelity of paleointensity results for the Thellier-Thellier type experiments because the unblocking temperatures of the newly-formed magnetic particles could be higher than the thermally treatment temperature (Zhao et al. 2014). However, such a flaw can be overcome by the room-temperature-dependent of magnetic parameters (e.g., ARM-T, SIRM-T). Upon the thermal treatment, two kinds of mineral transformations occur. The first type of alteration can produce newly-formed strongly magnetic minerals. Despite of the distribution of the unblocking temperatures, the enhanced concentration-dependent of magnetic parameters can sensitively detect the neoformation of magnetic minerals.

The second type of thermal alterations do not produce new minerals but can oxidize the primary magnetic minerals to a less magnetic state, e.g., from magnetite to maghemite, which could significantly decrease the saturation magnetization (also ARM and SIRM values). Then, the first type and second type of thermal alterations will decrease and enhance the estimated paleointensity values, respectively (Zhao et al. 2014). Therefore, Qin et al. (2011) adopted a new parameter names chemical index (CI), which can be defined e.g., by $M_{rs\_300\ °C}/M_{rs\_raw}$. Besides the conventional pTRM checks, CI values should be < 10%, which indicates weakly thermal alteration effects. Such a rationale is also applied to this new study.

Except for the thermal alteration effects, PSD/MD particles can also seriously distort the Arai-plot. Therefore, by combing these two techniques, we constructed a new correlation between $M_{rs–300\ °C}/M_{rs–raw}$

to $M_{rs–500\ ^{\circ}C}$/ $M_{rs–raw}$ with B_{cr}/B_c to check the possible effects of thermal alteration during heating in paleointensity results. Clearly, almost all samples of higher paleointensity have $B_{cr}/B_c > 3$ and CI > 10%. The average of the values satisfying this criterion is 33.73 ± 1.88 μT. It is rather close to the expected value. This strongly indicate that positive pTRM checks indeed cannot exclude a large amount of failure estimations, most possibly due to the mechanism put forward by Zhao et al. (2012) and Qin et al. (2011).

Our study provided a practical new criteria to determine the fidelity of the paleointensity especially for results with conventional positive checks. This raise a serious question for the existing paleointensity results from the geological history. We strongly suggest that domain state and thermal stability for samples should be systematically incorporated into the paleotiensity studies except for all conventional criteria.

5. Conclusions

We present paleointensity using a temperature dependence hysteresis parameters with modified Thellier experiments of IZZI protocol from the 1960 Kilauea lava. Only 9 samples of the 30 samples succeeded on the basis of the positive pTRM checks. However, a large proportion of the “successful” paleointensity results fail to predict the expected value. This strongly indicate that positive pTRM checks can’t completely exclude the failure results because the conventional pTRM check can’t detect the thermal alteration with the unblocking temperature of the newly-formed magnetic particles higher than the treated temperature. Therefore, we put forward that the combination of chemical index and domain state parameters should be used in the future study, especially for the older samples, to improve the fidelity of the paleointensity results.

Abbreviations

AF: alternating field; ARM: anhysteretic remanent magnetization; ChRM: characteristic remanent magnetization; DRM: depositional remanent magnetization; IRM: isothermal remanent magnetization; IGRF: International Geomagnetic Reference Field; IZZI-T method: Thellier method with the IZZI protocol for absolute paleointensity determination; MAD: maximum angular deviation; MD: Multi-domain; M_s: saturation magnetization; M_{rs}: saturation remanence; B_c: magnetic coercivity; B_{cr}: coercivity of remanence ; PTRM: partial thermal remanent magnetization; PSD: pseudo-single-domain; RPI: relative paleointensity determination; SD: single-domain; $T_{ub:}$ unbloking temperature; T_b: blocking temperature; TCRM: thermochemical remanent magnetization TRM: thermoremanent magnetization; VFTB: variable field translation balance.

Declarations

Acknowledgements

This study was supported by the National Science Foundation of China (41874078).

Authors’ contributions

Doohee Jeong: Writign and Editing; Qingsong Liu: Conceptualization, Writing and Editing, Funding acquisition; Yuhji Yamamoto: Methodology, Software; Yongjae Yu: Reviewing and Editing; Xiang Zhao: Software; Huafeng Qin: Methodology.

Funding

This study was supported by the National Science Foundation of China (41874078).

Availability of data and materials

Data are available on request by contacting QSL.

Competing interests

The authors declare that they have no competing interests.

Author details

[1]Centre for Marine Magnetism (CM[2]), Department of Ocean Science and Engineering, Southern University of Science and Technology, Shenzhen 518055, China

[2] Center for Advanced Marine Core Research, Kochi University, Nankoku 783-8502, Japan

[3] Department of Geology and Earth Environmental Science, Chungnam National University, Daejeon 34134, South Korea

[4] Research School of Earth Sciences, Australian National University, Canberra, Australian Capital Territory, Australia

[5] Palaeomagnetism and Geochronology Laboratory, Key Laboratory of Earth’s Deep Interior, Institute of Geology and Geophysics, Chinese Academy of Sciences, Beijing 100029, China

References

1. Aitken MJ, Allsop AL, Bussell GD, Winter MB (1988). Determination of the intensity of the Earth’s magnetic field during archaeological times: Reliability of the Thellier Thechnique. Reviews of Geophysics 26: 3-12. doi:10.1029/RG026i001p00003

2. Biggin AJ, Piispa EJ, Pesonen LJ, Holme R, Paterson GA, Veikkolainen T, Tauxe L (2015) Paleomagnetic field intensity variations suggest Mesoproterozoic inner-core nucleation. Nature, 526. doi:10.1038/nature15523
3. Calvo-Rathert M, Morales-Contreras J, Carrancho Á, Goguitchaichvili A (2016). A comparison of Thellier-type and multispecimen paleointneisty determinations on Pleistocene and historical lava flows from Lanzatore (Canary Islands, Spain). Geochemistry, Geophysics, Geosystems, 17: 3638-3654. doi:10.1002/2016GC006396
4. Channell JET, Xuan C, Hodell DA (2009). Stacking paleointensity and oxygen isotope data for the last 1.5 Myr (PISO-1500). Earth and Planetary Science Letters, 283: 14-23. doi:10.1016/j.epsl.2009.03.012
5. Coe R S (1967). Paleo-intensitues of the Earth's magnetic field determined from Tertiary and Quaternary rocks. Journal of Geophysical Research, 72: 3247-3262. doi:10.1029/JZ072i012p03247
6. Coe R S, Grommé C S, Menkinen E A (1978). Geomagnetic pleointensities from radiocarbon-dated lava flows on Hawaii and the question of the Pacific nondipole low. Journal of Geophysical Research, 83: 1740-1756. doi:10.1029/JB083iB04p01740
7. Coe R S, Riisager J, Plenier G, Leonhardt E, Krash D (2004). multidomain behavior during Thellier paleointensity experiments: result from the 1915 Mt. Lassen flow. Physics of the Earth and Planetary Interiors, 147 (2-3): 141-153. doi:10.1016/j.pepi.2004.01.010
8. Day R, Fuller M, Schmidt VA (1977). Hysteresis Properties of titanomagnetites: Grain-size and compositional dependence. Physics of Earth and Planetary Interiors, 13: 260-267. doi:10.1016/0031-9201(77)90108-X
9. Dunlop DJ (2002). Theory and application of the Day plot (M_{rs}/M_s versus H_{cr}/H_c) 2. Application to data ricks, sediments, and soils. Journal of Geophysical Research, 107. doi:10.1029/2001JB000486
10. de Groot LV, Béguin A, Kosters ME, van Rijsingen EM, Struijk ELM, Biggin AJ, Hurst EA, Langereis CG, Dekkers MJ (2015). High paleointensities for the Canary Island constrain the Levant geomagnetic high. Earth and Planetary Science Letters, 419: 154-167. doi:10.1016/j.epsl.2015.03.020
11. Henry B, Jordanova D, Jordanova N, Goff ML (2005) Transformations of magnetic mineralogy in rocks revealed by difference of hysteresis loops measured after stepwise heating: theory and case studies. Geophysical Journal International, 162: 64-78. dou:10.1111/j.1365-246X.2005.02644.x
12. Herrero-Bervera E, valet J -P (2009) Testing determinations of absolute paleointensity from the 1995 and 1960 Hawaiian flows. Earth and Planetary Science Letters, 287: 420-433. doi:10.1016/j.epsl.2009.08.035
13. Hill M J, Shaw J (2000) Magnetic field intensity study of the 1960 Kilauea lava flow, Hawaii, using the microwave paleointensity technique. Geophysical Journal International, 143: 487-504. doi:10.1046/j.1365-246x.2000.00164.x
14. Kirschvink J L (1980) The least-squares line and plane and the analysis of paleomagnetic data. Geophysical Journal International, 62: 699-718. doi:10.1111/j.1365-246X.1980.tb02601.x

15. Larson RL, Olson P (1991) Mantle plumes control magnetic reversal frequency. Earth and Planetary Science Letters, 107: 437-447. doi:10.1016/0012-821X(91)90091-U
16. Macouin M, Valet J -P, Besse J (2004) Long-term, evolution of the geomagnetic dipole moment. Physics of the Earth and Planetary Interiors, 147: 239-246. doi: 10.1016/j.pepi.2004.07.003
17. Morales J, Zhao X, Goguitchaichvili A (2010) Geomagnetic field intensity from Kilauea 1995 and 1960 lava flows: Towards a better understanding of paleointensity. Studia Geophysica et Geodaetica, 54: 561-574. doi:10.1007/s11200-010-0034-6
18. Olson P, Deguen R, Hinnov LA, Zhong S (2013) Controls on geomagnetic reversals and core evolution by mantle convection in the Phanerozoic. Physics of the Earth and Planetary Interiors, 214: 87-103. doi:10.1016/j.pepi.2012.10.003
19. Qin H, He H, Liu QS, Cai S (2011) Paleointensity just at the onset of the Cretaceous normal superchron. Physics of the Earth and Planetary Interiors, 187: 199-211. doi:10.1016/j.pepi.2011.05.009
20. Ritcher DH, Eaton JP, Murata KJ, Ault WU, Krivoy HL (1970) Chronological narrative of the 1959-60 eruption of Kilauea Volcano, Hawaii. USGS survey professional Paper, 537-E. doi:10.3133/pp537E
21. Rowland SK, Walker PL. George (1987) Toothpaste lava: Characteristic and origin of a lava structural type transitional between pahoehoe and aa, Bulletin of Volcanology, 49: 631-641. doi:10.1007/BF01079968
22. Selkin P, Tauxe L (2000). Long-term variations in paleointensity, Philisophical Transactions of the Royal Society A. 358. doi:10.1098/rsta.2000.0574
23. Tarduno J A, Cottrell RD, Watkeys MK, Bauch D (2007). Geomagnetic field strength 3.2 billion years ago recorded by single silicate crystals. Nature, 446. doi: 10.1038/nature05667
24. Tanaka H, Kono M (1991) Preliminary Results and Reliability of Paleointensity Studies on Historical and ^{14}C Dated Hawaiian Lavas. Journal of Geomagnetism and Geoelectricity, 43: 375-388. doi:10.5636/jgg.43.375
25. Tanaka H, Athanassopoulos JDE, Dunn JR, Fuller M (1995) Paleointensity Determinations with Measurements at High Temperature, Journal of Geomagnetism and Geoelectricity, 47: 103-113. doi:10.5636/jgg.47.103
26. Tauxe L (1993) Sedimentary records of relative paleointensity of the geomagnetic field: theory and practice, Reviews of Geophysics, 31: 319-354. doi:10.1029/93RG01771
27. Tauxe L, Staudigel H (2004) Strength of the geomagnetic field in the Cretaceous Normal Superchron: New data from submarine basaltic glass of the Troodos Ophiolite. Geochemistry, Geophysics, Geosystems, 5, Q02H06. doi:10.1029/2003GC000635
28. Thellier E (1938) Sur l'aminatation des teres cuites et ses applications g'eophysique, Annales de l'Institute physique dy Globe, Paris, 16: 157-302.
29. Thellier E, Thellier O (1959) Sur l'intensité de champ magnétique terrestre dans le passé historique et géologique, Annales de Géophysique, 15: 285-378.

30. Tsunakawa H, Shaw J (1994) The Shaw method of paleointensity determinations and its application to recent volcanic rocks. Geophysical Journal International, 118: 781-787. doi:10.1111/j.1365-246x.1994.tb03999.x
31. Valet J-P, Meynadier L, Guyodo Y (2005), Geomagnetic dipole strength and reversal rate over the past two milliom years. Nature, 435. doi:10.1038/nature03674
32. Valet J-P, Herrero-Bervera E. 2000, Paleointensity experiments using alternating field demagnetization. Earth and Planetary Science Letters, 177: 43-88. doi: 10.1016/S0012-821X(00)00036-4
33. Yamamoto Y, Tsunakawa H, Shibuya H (2003), Paleointensity study of the Hawaiian 1960 lava: implications for possible causes of erroneously high intensities. Geophysical Journal International, 153: 263-276. doi:10.1046/j.1365-246X.2003.01909.x
34. Yamazaki T, Oda H (2005), A geomagntic paleointensity stack between 0.9 and 3.0 Ma from equatorial Pacific sediment cores. Geochemistry, Geophysics, Geosystems, 6 (11), doi:10.1029/2005GC001001
35. York D (1969), Least squares fitting of a straight line with correlated errors, Earth and Planetary Science Letters, 5: 320-324. doi:10.1016/S0012-821(68)80059-7
36. Yu Y, Tauxe L, Genevey A. (2004), Toward an optimal geomagnetic field intensity determination technique. Geochemistry, Geophysics, Geosystems, 5 (2). doi: 10.1029/2003GC000630
37. Ziegler LB, Constable CG, Johnson CL, Tauxe L (2011), PADM2M: a penalized maximum likehood model of the 0-2 Ma paleomagnetic axial dipole moment. Geophysical Journal International, 184. doi:10.1111/j.1365-246X.2010.04905.x
38. Zhao XY, Liu QS, Paterson GA, Qin HF, Cai SH, Yu Y, Zhu RX (2014) The effects of secondary mineral formation on Coe-type paleointensity determinations: Theory and simulation. Geochemistry Geophysics Geosystems, 125: 1215-1234. doi:10.1002/2013GC005165.

Figures

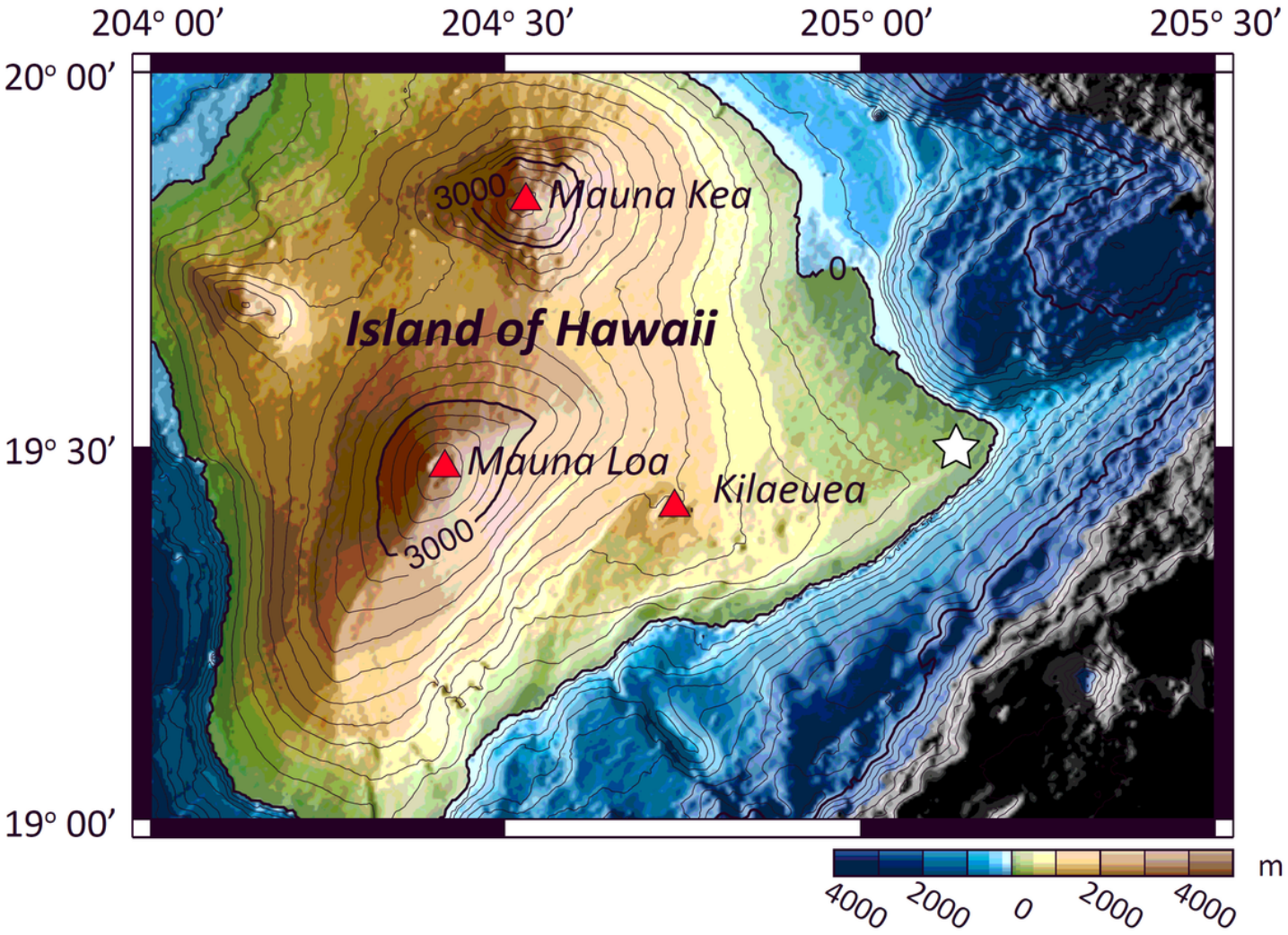

Figure 1

Location map of Island of Hawaii and sample location (star; 19° 30.43’N, 154° 50.46W).

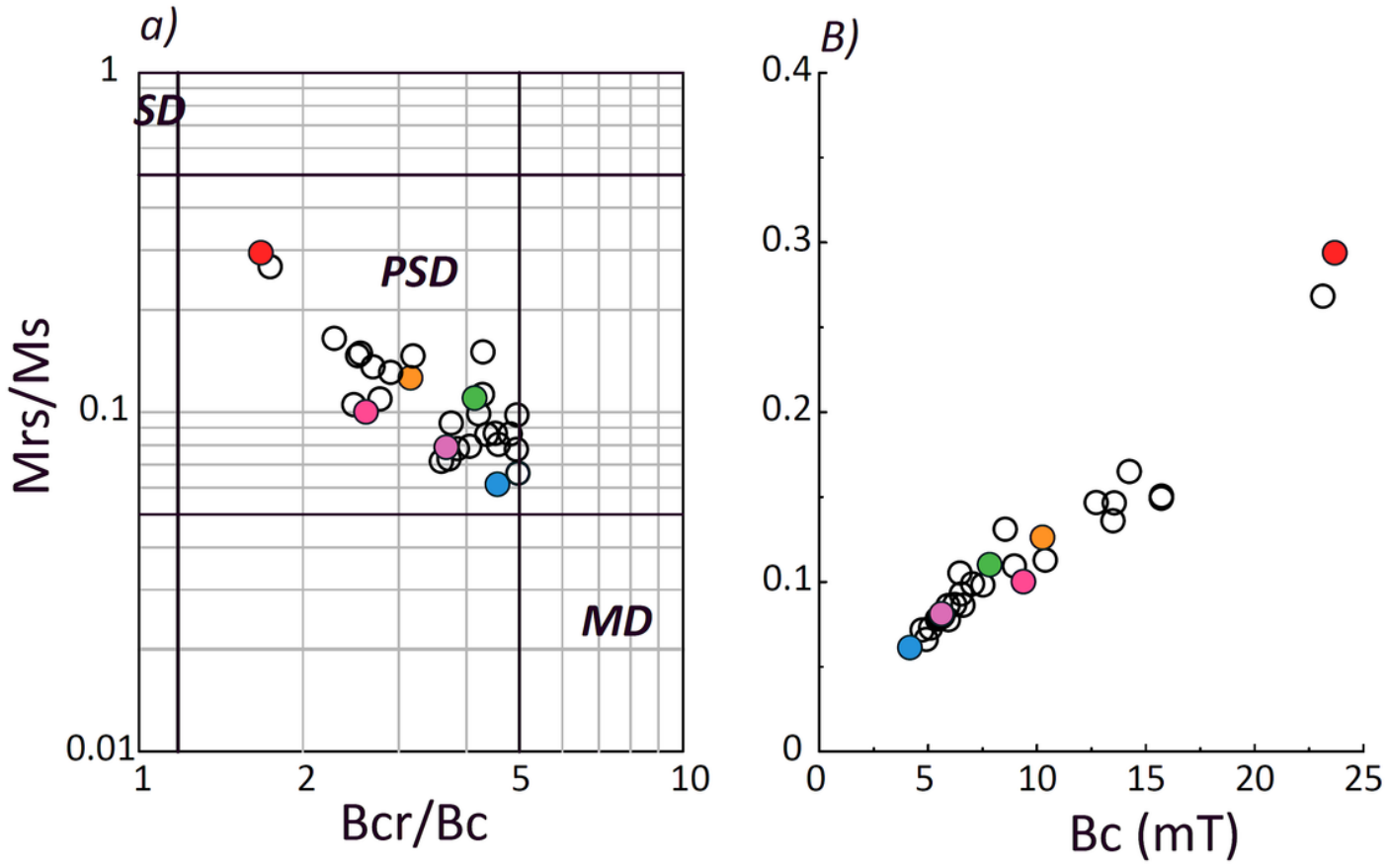

Figure 2

Hysteresis properties displayed in a) a Day plot, and b) a function of coercivity and remanence ratio.

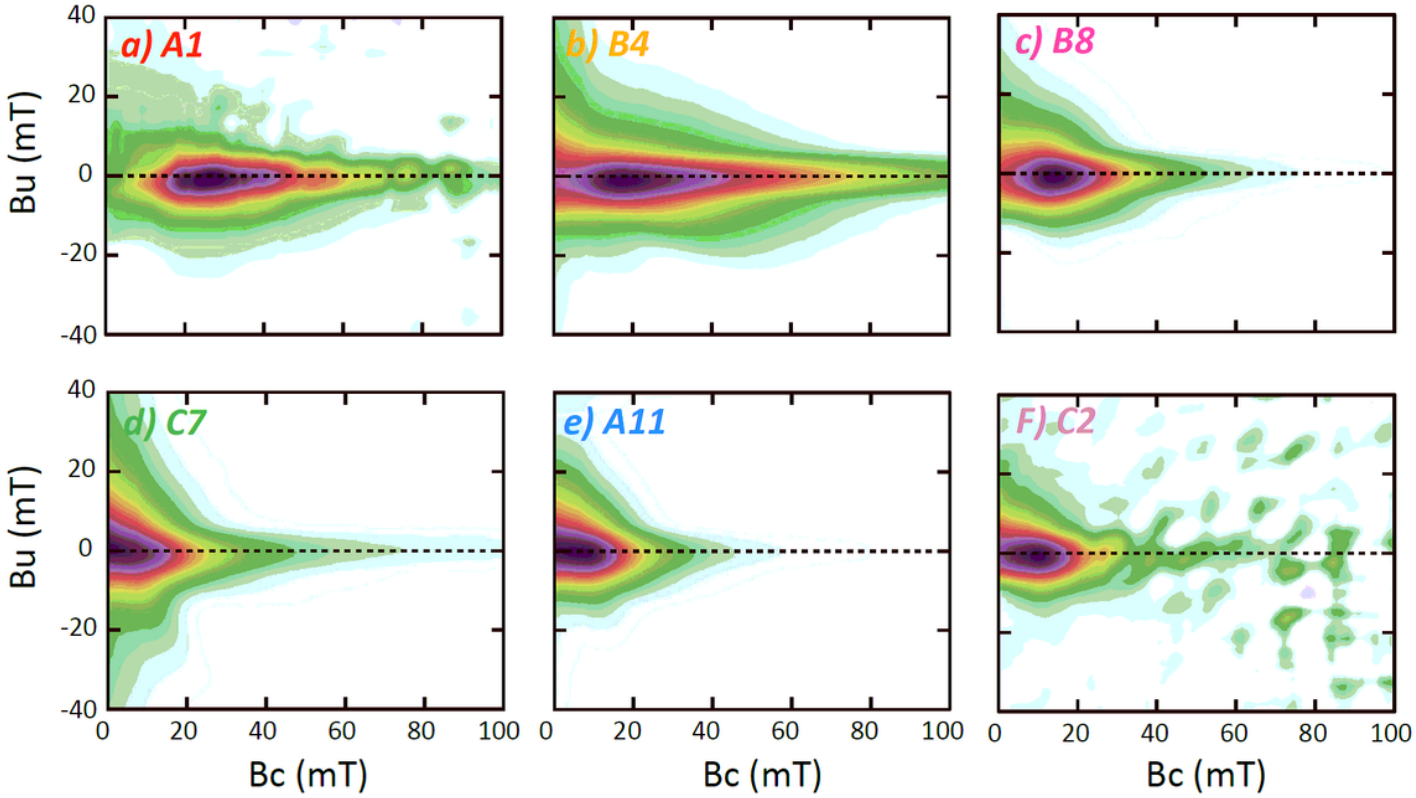

Figure 3

First order reversal curve (FORC) diagrams for representative samples (Smoothing factor=8).

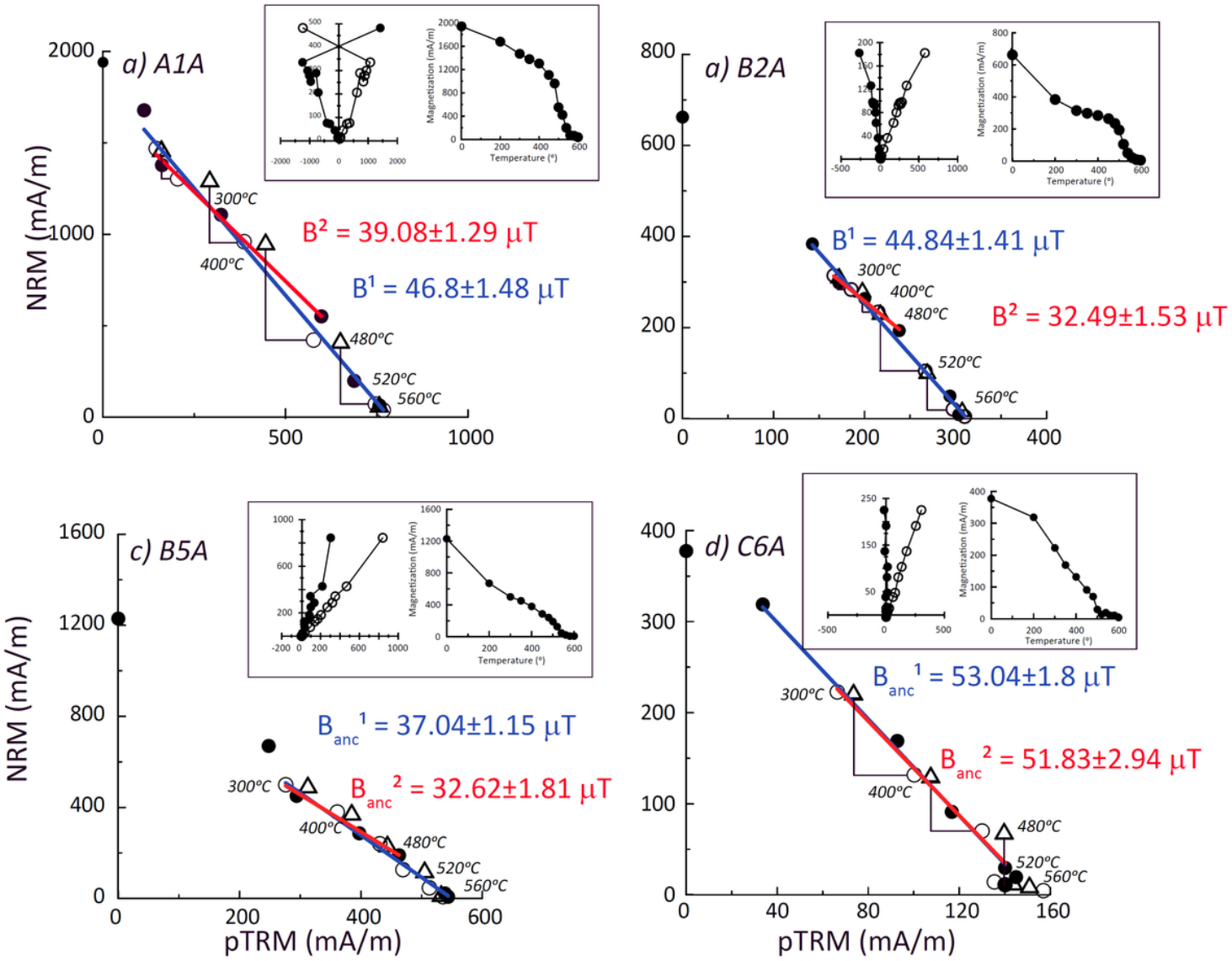

Figure 4

Display Arai plot illustrating successful paleointensity determinations for IZZI protocol (in-zero field step and zero-in field step with solid circles and open circles, respectively). pTRM checks (triagle) reproduce the origin pTRM within 5%. The inset are orthogonal vector plots with solid (open) correspond to horizontal (vertical) planes, extracted from zero-field steps and representative thermal demagnetization patterns.

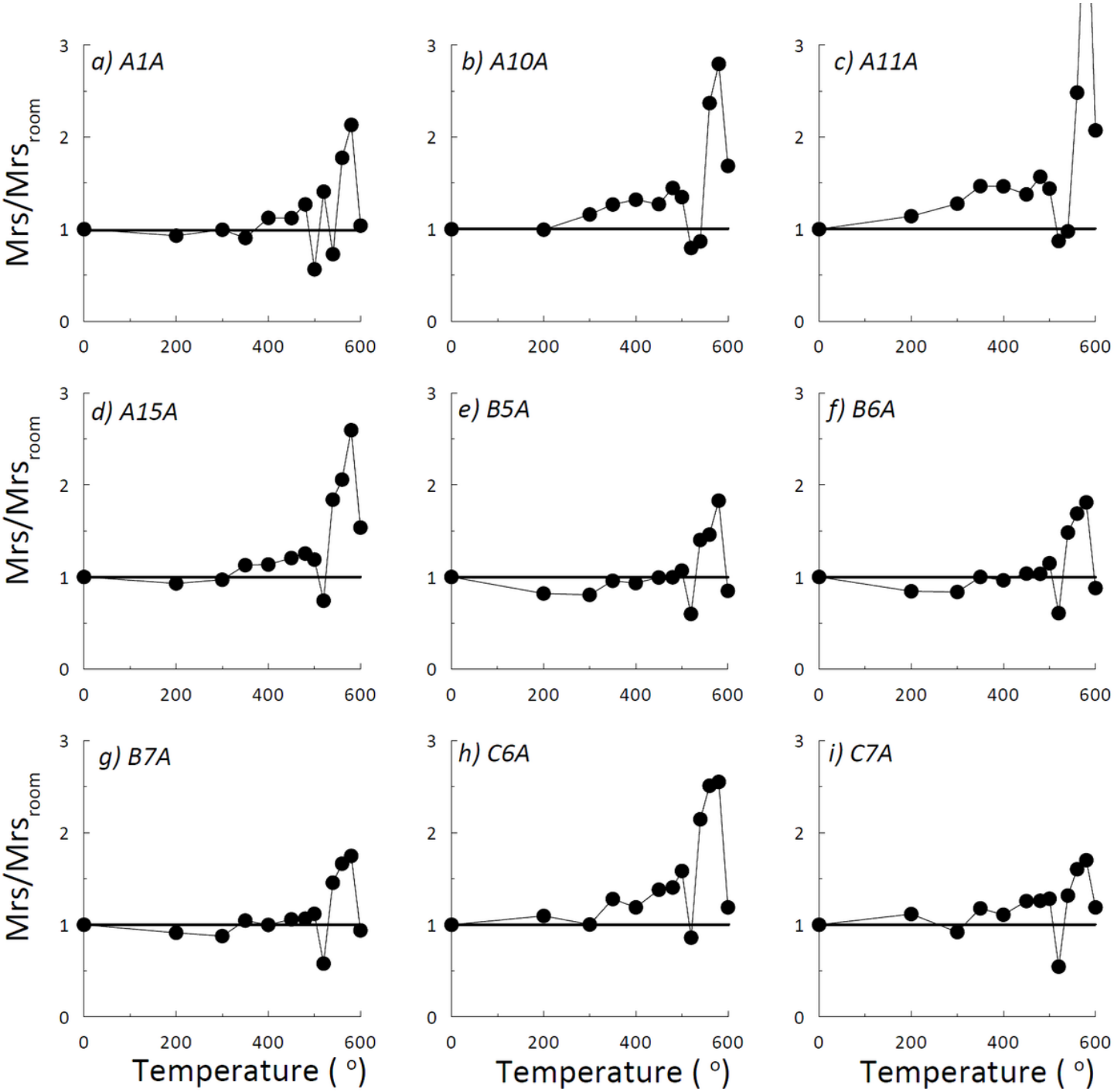

Figure 5

Representative normalized room temperature saturation remanence magnetization from all successful paleointensity samples.

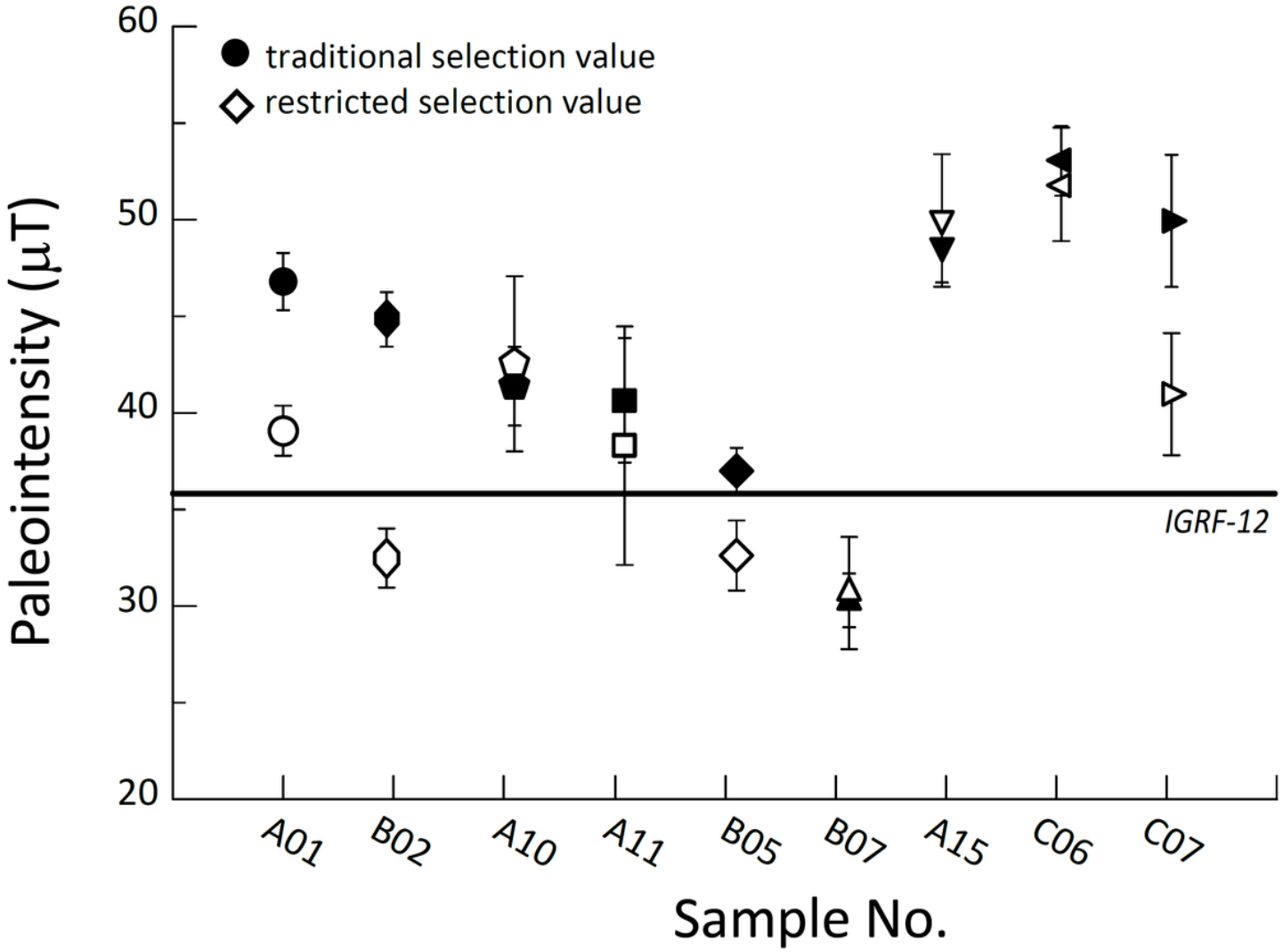

Figure 6

Display compare with traditional selection value between restricted selection value from each sample. The Horizontal line is IGRF-12 value at sampling site (36.1 μT) (grey box: 10% error).

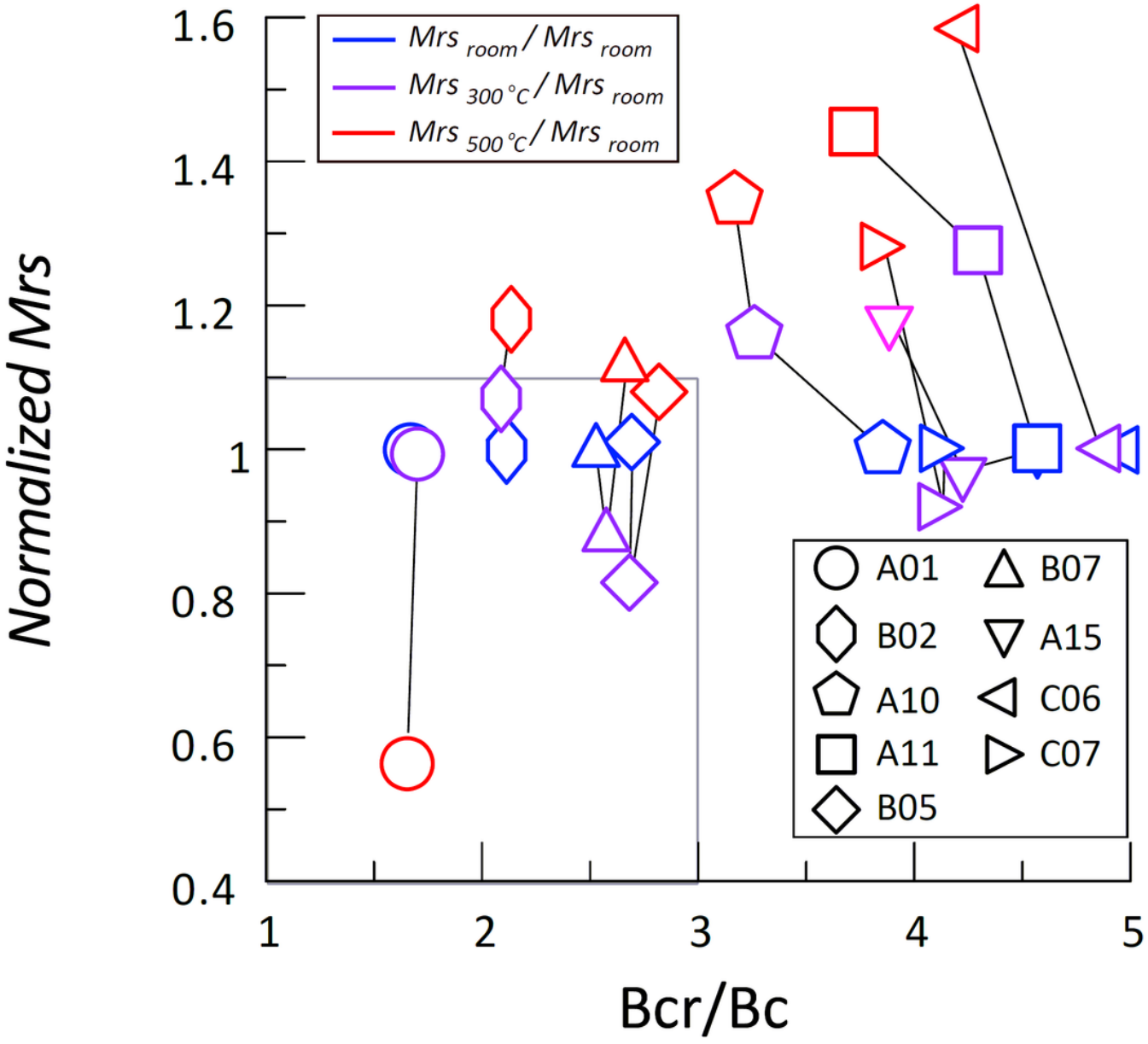

Figure 7

Plot of coercivity ratio versus the variation ratio of normalized saturation remanence at room temperature.

Supplementary Files

This is a list of supplementary files associated with this preprint. Click to download.

- Graphicabstract.png